Split-convexity method for image restoration

Hamdi Houichet* — Anis Theljani** — Badreddine Rjaibi* — Maher Moakher*

* Université de Tunis El Manar, Ecole Nationale d'Ingénieurs de Tunis,
Laboratoire de Modélisation Mathématique et Numérique dans les Sciences de l'Ingénieur
B.P. 37, 1002 Tunis, Tunisia.
hamdi.houichet@enit.utm.tn (H. Houichet), badreddine.rjaibi@lamsin.rnu.tn (B. Rjaibi),
maher.moakher@enit.utm.tn (M. Moakher).
** Liverpool Centre for Mathematics in Healthcare, Department of Mathematical Sciences, University of Liverpool, Liverpool, UK.
A.Theljani@liverpool.ac.uk

ABSTRACT. Image processing such as image denoising, edge detection and image segmentation, etc, plays an important role in various fields. The objective of image denoising is to reconstruct an original image from a noisy one. In this talk, we propose a nonlinear equation based on the $p(\cdot)$-biharmonic operator to denoise the images. First, we consider a topological gradient approach in order to detect important objectes of the image. Then, we chose the variable exponent $p(\cdot)$ adaptively based on the map furnished by the topological gradient. Finally, we consider the split convexity method in order to linearize the proposed equation. We present some numerical examples to show the performance of the proposed method.

RÉSUMÉ. Le traitement d'images tel que le débruitage, la détection de contour et la segmentation, etc., jouent un rôle important dans divers domaines. L'objectif du débruitage d'image est de reconstruire une image originale à partir d'une image bruitée. Dans cet exposé, nous proposons un modèle non linéaire basé sur l'opérateur $p(\cdot)$-biharmonic pour restaurer les images. Premièrement, nous considérons une approche de gradient topologique afin de détecter les importants objets de l'image. Ensuite, nous avons choisi la variable $p(\cdot)$ en fonction du gradient topologique. Finalement, nous considérons la méthode de la décomposition convexe afin de linéariser le modèle proposé. Nous présentons quelques exemples numériques pour montrer la performance de la méthode proposée.

KEYWORDS : variational method, image denoising, biharmonic operator, topological gradient, speckle noise, nonlinear PDE.

MOTS-CLÉS : Méthode variationnelle, débruitage d 'image, opérateur biharmonique, gradient topologique, bruit de type speckle, EDP non linéaire.

1. Introduction

In this work, we are interested in the restoration of images highly corrupted with multiplicative noise. The objective of image denoising is to reconstruct an image $u : \Omega \subset \mathbb{R}^2 \to \mathbb{R}$ from an observed one $f : \Omega \to \mathbb{R}$ which is degraded and contaminated by noise. The degradation model that we consider is the following:

$$f = u + \eta\sqrt{u}, \tag{1}$$

where $\eta : \Omega \to \mathbb{R}$ is a positive function and that follows the Rayleigh-distribution. Model (1) represents the degradation of an image corrupted by speckle noise, usually present in medical ultrasound imaging [5, 6]. We consider the following partial deferential equation for denoising the ultrasound image:

$$\begin{cases} \Delta^2_{p(x)} u + \alpha \frac{u^2 - f^2}{u^2} = 0, & \text{in } \Omega, \\ \partial_n \Delta u = \partial_n u = 0, & \text{on } \partial\Omega, \end{cases} \tag{2}$$

where $\Delta^2_{p(x)} u := \Delta(|\Delta u|^{p(x)-2} \Delta u)$ is the $p(\cdot)$-biharmonic operator, $p : \Omega \to]1, 2]$ is measurable function called exponent and α is a positive parameter. For more details about the exponent functions, we refer the reader to [3, 7].

The variable exponent $1 < p(x) \leq 2$ is chosen so that to slow diffusion near edges in order to highlight them, and to enhance diffusion in smooth regions. A classical idea of choosing the values of the exponent p is to make an adaptive procedure as follows: first, we consider the topological gradient method with $p(x) = 2$ to identify the edges in order to preserve them. Second, we perform a local selection of the exponent $1 < p(x) \leq 2$ with the help of the map furnished by the topological gradient.

2. Well-posedness

Let Ω be a bounded and Lipschitz open subset in $\mathbb{R}^2$. In the following theorem, we establish the well-posedness of equation (2).

Theorem 2.1. *Let $f \in X = \{u \in W^{2,p(x)}(\Omega)$ such that $\frac{\partial u}{\partial n} = 0$ on $\partial\Omega\}$ with $\inf_\Omega f > 0$. Then, equation* (2) *admits a unique solution u in X satisfying the maximum principal*

$$\inf_\Omega f \leq u \leq \sup_\Omega f.$$

Proof. First, we note that (2) is the Euler-Lagrange equation of the following minimization problem

$$\min_{\{u \in X, u > 0\}} \left\{ E_{p(x)}(u) := \int_\Omega |\Delta u|^{p(x)} \, \mathrm{d}x + \alpha \int_\Omega \frac{(f-u)^2}{u} \, \mathrm{d}x \right\}. \tag{3}$$

By the classical compactness, semi-continuity and convexity arguments of the energy $E_{p(x)}(\cdot)$, it is easy to verify that (3) has a unique minimizer, which is equivalently the unique weak solution of (2). □

3. Edges-detection and preservation

The big challenge in image restoration and segmentation problems is how to accurately detect features such as arteries, filaments, internal organ, etc. To meet with this challenge, we employ here the topological gradient method which was widely used in edge detection [1, 5]. We start by inserting a small crack $\sigma_\varepsilon := \{x_0 + \varepsilon\sigma(n)\}$ in the domain Ω, where $x_0 \in \Omega$, $\varepsilon > 0$, $\sigma(n)$ is a straight crack, and n is a unit vector normal to the crack and we minimize the cost function

$$j(\Omega_\varepsilon) := J(u_\varepsilon) = \int_{\Omega\setminus\sigma_\varepsilon} |\Delta u_\varepsilon|^2 \, \mathrm{d}x,$$

where u_ε is the unique solution of the following equation defined on the *perturbed domain* $\Omega_\varepsilon \overset{\text{def}}{=} \Omega \setminus \overline{\sigma}_\varepsilon$:

$$\begin{cases} \Delta^2 u_\varepsilon + \alpha \frac{u_\varepsilon^2 - f^2}{u_\varepsilon^2} = 0, & \text{in } \Omega_\varepsilon, \\ \frac{\partial \Delta u_\varepsilon}{\partial n} = \frac{\partial u_\varepsilon}{\partial n} = 0, & \text{on } \partial\Omega, \\ \frac{\partial \Delta u_\varepsilon}{\partial n} = \Delta u_\varepsilon = 0, & \text{on } \partial\sigma_\varepsilon. \end{cases} \tag{4}$$

After that, we measure the impact of such a modification of the domain on this cost function by computing the following asymptotic expansion as ε goes to zero

$$J(u_\varepsilon) - J(u_0) = \rho^2 G(x_0, n) + o(\rho^2),$$

where $G(x_0, n)$ is the topological gradient given by [1, 5]:

$$G(x_0, n) = -\pi \Delta u_0(x_0) \cdot (n, n) \Delta v_0(x_0)(n, n), \tag{5}$$

and v is the solution of the adjoint problem

$$\begin{cases} \Delta^2 v + \alpha \frac{2f^2}{u^3} v = -\Delta^2 u, & \text{in } \Omega, \\ \frac{\partial \Delta v}{\partial n} = \frac{\partial v}{\partial n} = 0, & \text{on } \partial\Omega. \end{cases} \tag{6}$$

4. Numerical computation

4.1. Split convexity method

However, for such a choice of $p(\cdot)$, equation (2) is strongly nonlinear. For that, we introduce an artificial time variable t and for any fixed number T, we transform our problem to the following time-dependent one:

$$\begin{cases} u_t = -\nabla E_{p(\cdot)}(u), & \text{in } \Omega \times (0,T], \\ u(.,t=0) = f, & \text{in } \Omega, \end{cases} \tag{7}$$

where $\nabla E_{p(\cdot)}(u)$ denotes the Gateaux derivative of $E_{p(\cdot)}(\cdot)$ about u.

After that, we consider *the split convexity* method (see [2, 4]) to solve problem (7). The basic idea of this method is to split the functional $E_{p(\cdot)}$ into a convex part treated implicitly, and a concave one treated explicitly. In our case, we split the energy $E_{p(\cdot)}$ as follows:

$$E_{p(\cdot)} = E_{1,2} - E_{2,p},$$

where

$$\begin{cases} E_{1,2} = \frac{c_1}{2}\int_\Omega |\Delta u|^2 \,\mathrm{d}x + \frac{c_2}{2}\int_\Omega |u|^2 \,\mathrm{d}x, \\ E_{2,p} = -\int_\Omega \frac{1}{p(x)}|\Delta u|^{p(x)} \,\mathrm{d}x - \alpha\int_\Omega \frac{(f-u)^2}{u} \,\mathrm{d}x + \frac{c_1}{2}\int_\Omega |\Delta u|^2 \,\mathrm{d}x + \frac{c_2}{2}\int_\Omega |u|^2 \,\mathrm{d}x, \end{cases}$$

and c_1 and c_2 are two positive constants. Let τ be the time-step, and write $t_k = k\tau$, $u^k(x) = u(x,t_k)$, with $k = 1, 2, \dots, [T/\tau] - 1$, then, the resulting discrete time stepping scheme for an initial condition u^0 is is given by

$$\frac{u_{k+1} - u_k}{\delta t} + c_1\Delta\Delta u_{k+1} + c_3 u_{k+1} = -\Delta^2_{p(x)} u_k + c_1\Delta\Delta u_k + c_3 u^k - \alpha\frac{u_k^2 - f^2}{u_k^2}. \tag{8}$$

We use Neumann boundary conditions on $\partial\Omega$:

$$\frac{\partial u_k}{\partial n} = \frac{\partial \Delta u_k}{\partial n} = 0.$$

4.2. Algorithm

The steps of the restoration algorithm are the following:

Algorithm 1 MAIN ALGORITHM

Given f and α.

1) For $p(\cdot) \equiv 2$, compute u and v which solve equations (4) and (6), respectively.
2) Compute the topological gradient $G(x_0, n)$ for each point $x_0 \in \Omega$.
3) Update $q(\cdot)$ as function on $G(x_0, n)$ to obtain a new exponent and solve (8).

In order to update to exponent $p(\cdot)$, we use the following formula

$$p_a(x) = 1 + \exp(-\mu|G(x, n)|), \ \forall x \in \Omega,$$

where $\mu > 0$ is a constant.

4.3. Results

We present here some numerical results in order to show the efficiency of our method. In Figure 1(c), we observe that the blood vessels are well detected by the topological gradient method. The main difference between the noisy image (Figure 1(b)) and restored one (Figure 1(b)) is compared quantitatively by using the SNR and SSIM indicators. The segmented image is presented in Figure 1(d). We remark that all the regions of the image are well identified.

This remark holds true for the synthetic image presented in Figure 2.

5. References

[1] A. Drogoul, *Numerical analysis of the topological gradient method for fourth order models and applications to the detection of fine structures in imaging*, SIAM Journal on Imaging Sciences, vol. 7, pp. 2700–2731, 2016.

[2] D. J. Eyre, *Unconditionally gradient stable time marching the Cahn-Hilliard equation*, MRS Proceedings, vol. 529, Cambridge Univ. Press (1998), p. 39.

[3] X. Fan and D. Zhao, *On the spaces $L^{p(x)}(\Omega)$ and $W^{m,p(x)}(\Omega)$*, J. Math. Anal. Appl., vol. 263, pp. 424–446, 2001.

[4] K. Glasner and S. Orizaga, *Improving the accuracy of convexity splitting methods for gradient flow equations*, Journal of Computational Physics, vol. 315, pp. 52–64, 2016.

[5] H. Houichet, A. Theljani, B. Rjaibi and M. Moakher, *A nonstandard higher-order variational model for speckle noise removal and thin-structure detection*, submitted to International Journal of Computer Mathematics, p. 31, 2018.

[6] K. Krissian, R. Kikinis, C.-F. Westin, and K. Vosburgh, *Speckle-constrained filtering of ultrasound images*, in 2005 IEEE Computer Society Conference on Computer Vision and Pattern Recognition (CVPR'05), vol. 2, pp. 547–552, 2005.

[7] A. Zang and Y. Fu, *Interpolation inequalities for derivatives in variable exponent Lebesgue-Sobolev spaces*, Nonlinear Anal., vol. 69, pp. 3629–3636, 2008.

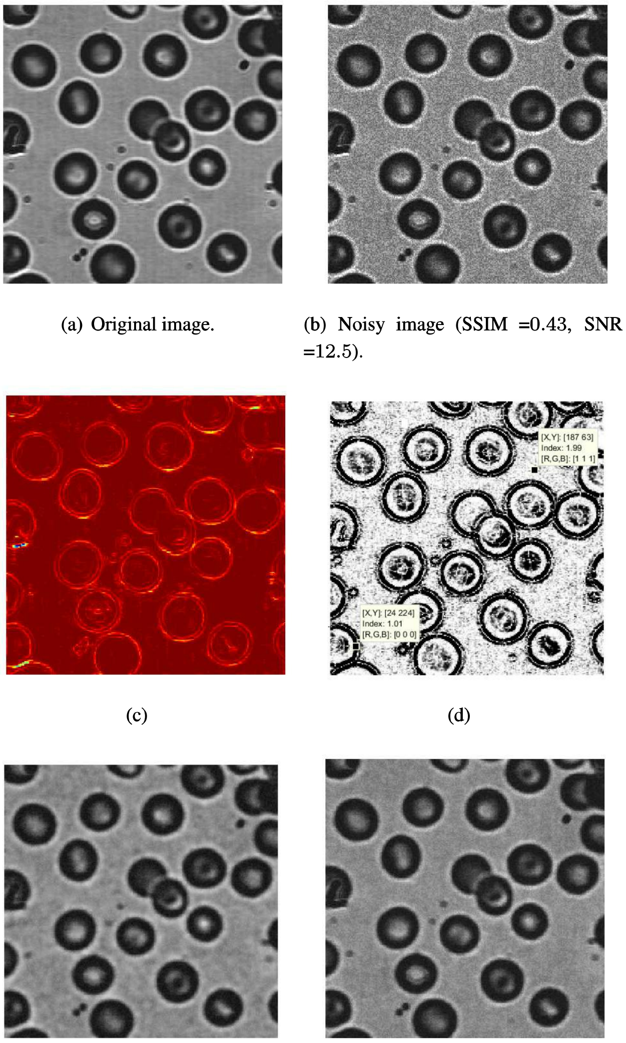

(a) Original image.

(b) Noisy image (SSIM =0.43, SNR =12.5).

(c)

(d)

(e) biharmonic model (SSIM=0.76, SNR=18.95dB)

(f) $p(\cdot)$-biharmonic model (SSIM =0.81, SNR =18.93).

Figure 1. *From left to right and top to bottom: (a) Original image, (b) Noisy image, (c) Topological gradient , (d) The variable exponent $p(\cdot)$ (e) biharmonic model and (f) $p(\cdot)$-biharmonic model.*

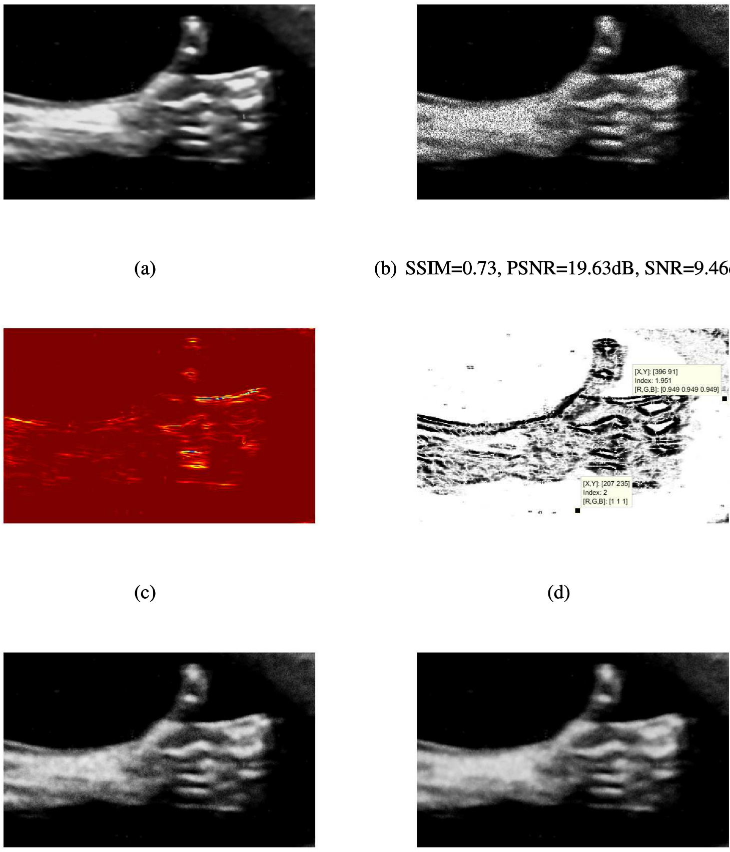

(a)

(b) SSIM=0.73, PSNR=19.63dB, SNR=9.46dB

(c)

(d)

(e) SSIM=0.93, PSNR=27.77dB, SNR=17.47dB

(f) SSIM=0.94, PSNR=30.6dB, SNR=20.31dB

Figure 2. *From left to right and top to bottom: (a) Original image, (b) Noisy image, (c) Topological gradient , (d) The variable exponent $p(\cdot)$ (e) biharmonic model and (f) $p(\cdot)$-biharmonic model.*